



SARAO
South African Radio
Astronomy Observatory

Snapshot Observations with MeerKAT

Document number: M2600-0000-037
Revision: 1
Classification: Public
Prepared by: T. Mauch, T. Jarrett, W. D. Cotton, J. J. Condon
Date: July 9, 2020

Organisation	:	NRF (National Research Foundation)
Facility	:	SARAO (South African Radio Astronomy Observatory)
Project	:	MeerKAT
Document Type	:	Report
Function/Discipline	:	Science commissioning

Document Approval

	Name	Designation	Affiliation	Signature/Date
Submitted by	T. Mauch	Science Processing Developer	SARAO	

Document History

Revision	Date of Issue	Person Responsible	Comments
1	9 July 2020	T. Mauch	First Version

Document Software

	Package	Version	Filename
Stylesheet	katscidoc	3.0	katscidoc.sty
Word processor	L ^A T _E X		

Organisation Details

Name	SARAO Johannesburg Office (Rosebank, Gauteng)	SARAO, Cape Town Office (Observatory, Cape Town)	SARAO HartRAO (Hartebeesthoek, Gauteng)	SARAO, Karoo Astronomy Reserve (Carnarvon, Northern Cape)
Physical / Postal Address	1 st Floor, 17 Baker Street Rosebank, Gauteng 2196, South Africa	2 Fir Street (North Entrance) Black River Park, Observatory Cape Town, 7925	PO Box 443 Krugersdorp 1740, South Africa	Posbus 69 Carnarvon 8925, South Africa
Tel.	+27 11 268 3400	+27 21 506 7300	+27 12 301 3100	+27 21 506 7300
Fax	+27 11 442 2454	+27 21 506 7375	+27 12 301 3300	+27 86 538 6836
Website	http://www.ska.ac.za	http://www.ska.ac.za	http://www.ska.ac.za	http://www.ska.ac.za

Contents

1	Abstract	5
2	MeerKAT Snapshot Observations of 122 Southern Galaxies	5
3	MeerKAT's Snapshot Survey Speed	8

List of Figures

- 1 The 122 target sources are scattered over the southern hemisphere. The dashed green line at J2000 $\delta \approx -30^\circ 43'$ marks the MeerKAT zenith declination. Sources north and south of this line were observed in separate groups to avoid long azimuth slew times. 5
- 2 Left panel: The inner $8' \times 8'$ of the MeerKAT 1.28 GHz continuum image of NGC 6156 restored with a $\theta_{1/2} \approx 7''.4$ FWHM Gaussian CLEAN beam. The intensity scale bar ranges from -0.1 to $+10 \text{ mJy beam}^{-1}$. Right panel: The off-source image fluctuations have rms $\sigma_I = 15 \mu\text{Jy beam}^{-1}$ 6
- 3 Left panel: This MeerKAT snapshot image targeting the galaxy NGC 1672 at J2000 $\alpha = 04^{\text{h}} 45^{\text{m}} 42.^{\text{s}}.5$, $\delta = -59^\circ 14' 50''$ has been degraded by radial residual sidelobes from the $S \approx 1.3 \text{ Jy}$ background source PKS 0443–59 at J2000 $\alpha = 04^{\text{h}} 44^{\text{m}} 14.^{\text{s}}.4$, $\delta = -59^\circ 24' 53''$. The rms image fluctuation near NGC 1672 is $\sigma_I \approx 40 \mu\text{Jy beam}^{-1}$. The intensity scale bar goes from -0.1 to $+10 \text{ mJy beam}^{-1}$. Right panel: The probability distribution $P(\sigma_I)$ of Stokes I image fluctuations σ_I among the 122 snapshot observations starts near the rms thermal noise $\sigma_I \approx \sigma_V = 14 \mu\text{Jy beam}^{-1}$ and has a long positive tail caused by residual sidelobes of strong sources in the primary beam. 7

List of Tables

List of Abbreviations

Snapshot Observations with MeerKAT: A Commissioning Report

T. Mauch (SARAO), T. Jarrett (UCT)¹, W. D. Cotton (NRAO)², J. J. Condon (NRAO)²

1 Abstract

MeerKAT's low system noise and excellent instantaneous (u,v) coverage allow it to produce continuum images with FWHM resolution $\theta_{1/2} \approx 7.''5$, rms noise plus confusion $\sigma_1 \approx 15 \mu\text{Jy beam}^{-1} \approx 0.2\text{K}$, and dynamic range $\text{DR} \sim 30,000:1$ from a few short "snapshot" observations, thus enabling useful continuum observations of $\gtrsim 60$ target sources per day. MeerKAT's large primary beam solid angle $\Omega_{\text{pb}} \approx 1.41 \text{ deg}^2$ at 1.28 GHz also makes MeerKAT very competitive for making fast "blind" snapshot sky surveys covering solid angles $\Omega \gg \Omega_{\text{pb}}$. This commissioning report describes MeerKAT's snapshot sensitivity, dynamic range, and survey speed based on results from our recent 1.28 GHz snapshot observations of 122 bright star-forming galaxies, and it provides a foundation for MeerKAT users to plan and execute future snapshot observing programs.

2 MeerKAT Snapshot Observations of 122 Southern Galaxies

We made 1.28 GHz snapshot observations of 122 southern-hemisphere galaxies selected from the *IRAS* Revised Bright Galaxy sample (Sanders et al. 1988) during $6 \times 8^{\text{h}}$ observing sessions in 2020 May and June. The sky distribution of these galaxies is shown in Figure 1.

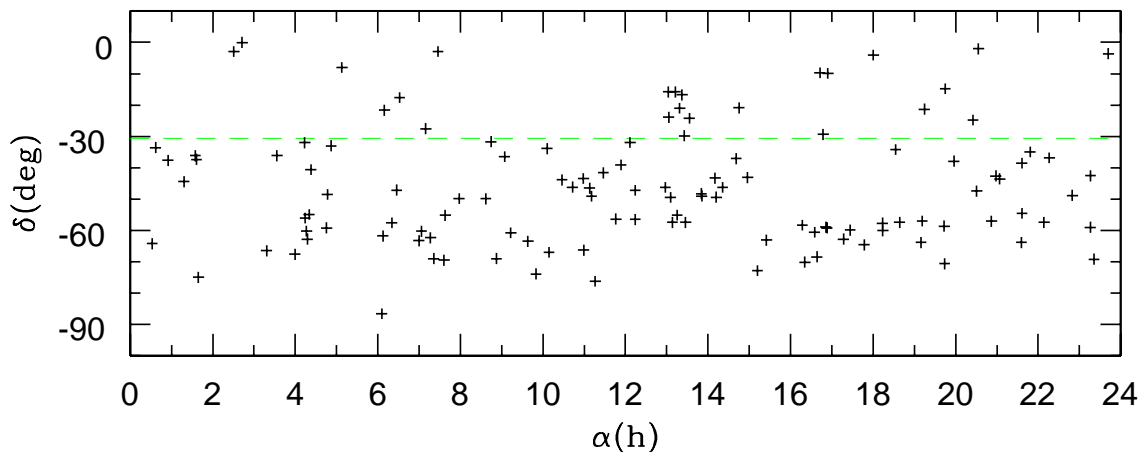


Figure 1: The 122 target sources are scattered over the southern hemisphere. The dashed green line at J2000 $\delta \approx -30^\circ 43'$ marks the MeerKAT zenith declination. Sources north and south of this line were observed in separate groups to avoid long azimuth slew times.

The sources were separated into small groups each assigned a single complex gain (amplitude and phase) calibrator, and every group plus its calibrator was observed in several cycles. Observing each source with five or six widely spaced 3 min snapshots improves its (u,v) coverage, helps to make a more nearly circular restoring beam, and insures against a complete loss of data caused by a short-term observing failure. The cost of making multiple short snapshots instead of a single longer snapshot is more time spent on slewing.

¹Astronomy Department, University of Cape Town, Private Bag X3, Rondebosch 7701, South Africa

²National Radio Astronomy Observatory, 520 Edgemont Road, Charlottesville, VA 22903, USA

Bandpass calibrator(s) were observed for 10 minutes every 2 hours, and a group complex-gain calibrator was observed for 1 minute per ~ 7 target scans. An individual target may be separated from its group complex-gain calibrator by a large fraction of a radian on the sky, so the external phase calibration may leave unacceptably large phase errors. We used two or three rounds of phase self-calibration to reduce these phase errors and increase image dynamic range. Including overheads for slewing and calibration, the average array time per target source was 23.6 min. The on-source integration times ranged from 15 to 18 min for an average on-target observing efficiency $\eta \approx 70\%$.

The first galaxy we observed was the $\log(L/L_\odot) = 11.14$ Luminous InfraRed Galaxy (LIRG) NGC 6156. The left panel in Figure 2 shows the central $8' \times 8'$ of its 1.28 GHz MeerKAT total-intensity (Stokes I) image, and the right panel shows the distribution of Stokes I image fluctuations near the target source. Its rms $\sigma_1 = 15 \mu\text{Jy beam}^{-1}$ includes contributions from pure thermal noise, confusion by numerous very

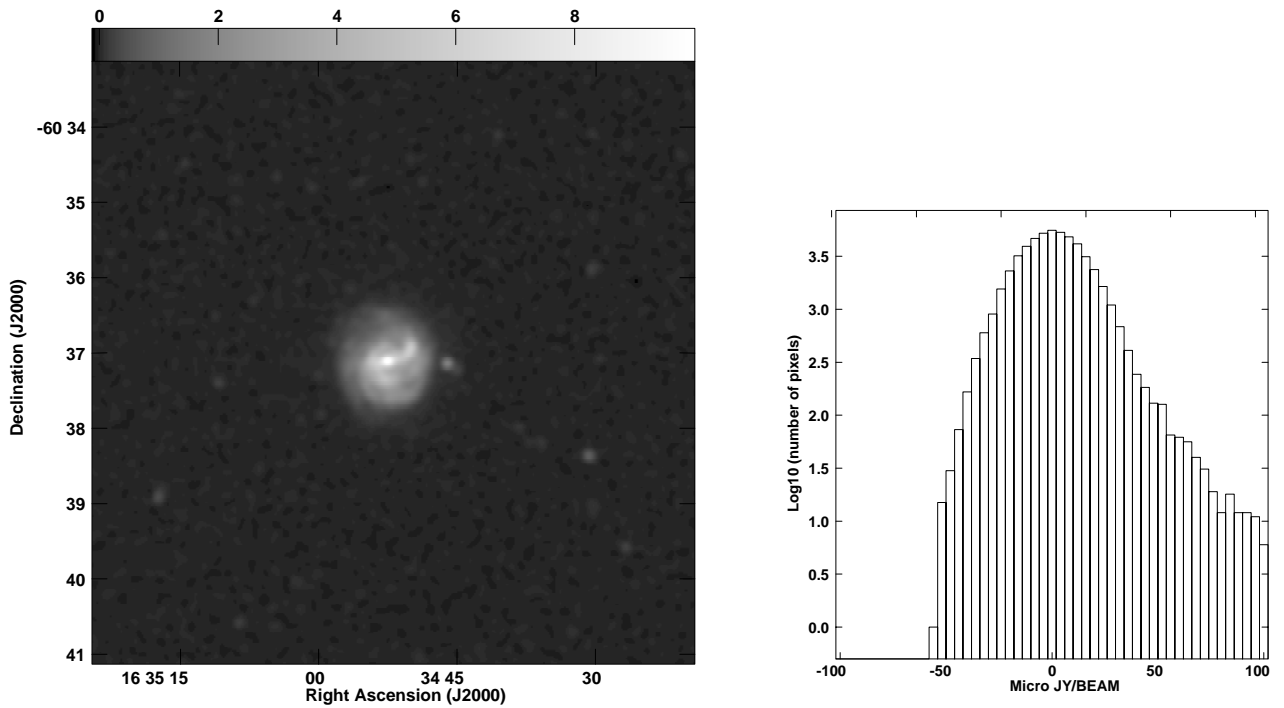


Figure 2: Left panel: The inner $8' \times 8'$ of the MeerKAT 1.28 GHz continuum image of NGC 6156 restored with a $\theta_{1/2} \approx 7''.4$ FWHM Gaussian CLEAN beam. The intensity scale bar ranges from -0.1 to $+10 \text{ mJy beam}^{-1}$. Right panel: The off-source image fluctuations have rms $\sigma_1 = 15 \mu\text{Jy beam}^{-1}$.

faint sources, and residual sidelobes from strong background sources in the primary beam. The median rms fluctuation $\sigma_V = 14 \mu\text{Jy beam}^{-1}$ in the Stokes V image is a good estimate of the pure thermal noise because most sources emit little circularly polarized flux. The confusion by faint sources has such a long tail that it is not well described by its rms, but it is $\sigma_1 \ll 14 \mu\text{Jy beam}^{-1}$ (Mauch et al. 2020) and small enough to be ignored in our snapshots. Finally, even after CLEANing, residual sidelobes from one or more strong sources anywhere in the primary beam may significantly increase the off-source image fluctuations; such images are limited more by dynamic range than by noise.

The CLEAN restoring beam is a nearly circular Gaussian with half-power diameter $\theta_{1/2} \approx 7''.4$ and beam solid angle

$$\Omega_b = \frac{\pi \theta_{1/2}^2}{4 \ln 2} \approx 62.0 \text{ arcsec}^2 \approx 1.46 \times 10^{-9} \text{ sr} . \quad (1)$$

The brightness temperature T_b at frequency $\nu = 1.28 \text{ GHz}$ corresponding to peak flux density S_p is

$$T_b = \frac{c^2 S_p}{2k\nu^2 \Omega_b} . \quad (2)$$

In units relevant to MeerKAT snapshot observations,

$$\left(\frac{T_b}{\text{K}} \right) \approx 0.20 \left(\frac{S_p}{15 \mu\text{Jy beam}^{-1}} \right) \left(\frac{7''.4}{\theta_{1/2}} \right)^2 \left(\frac{1.28 \text{ GHz}}{\nu} \right)^2 . \quad (3)$$

Note that $\sigma_1 \approx 15 \mu\text{Jy beam}^{-1} \approx 0.2 \text{ K}$ is sufficient to detect typical spiral galaxies, whose median face-on brightness temperature averaged over the optical disk is only $\langle T_b \rangle \sim 1.3 \text{ K}$ at 1.28 GHz .

Critical questions for MeerKAT snapshot observations are: “What is the typical dynamic range?” and “What fraction of fields is likely to be limited by dynamic range instead of noise?”

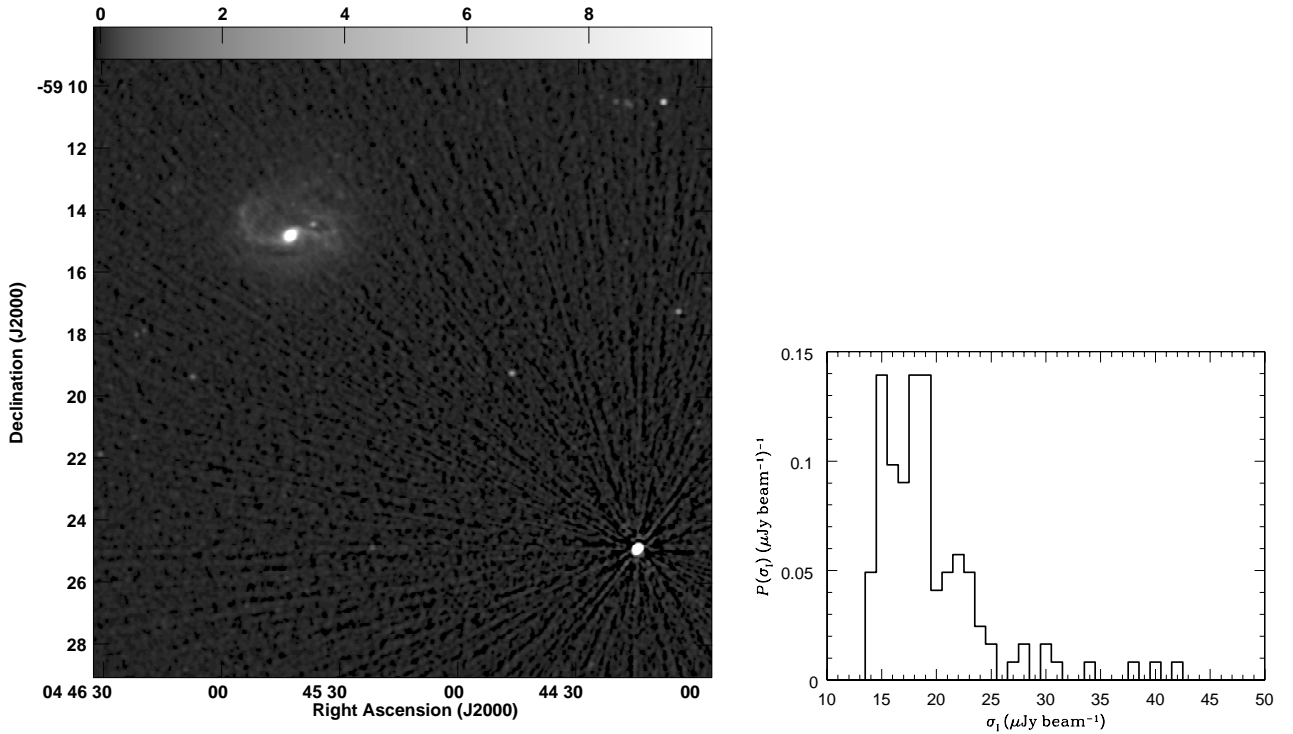


Figure 3: Left panel: This MeerKAT snapshot image targeting the galaxy NGC 1672 at J2000 $\alpha = 04^{\text{h}} 45^{\text{m}} 42.^{\text{s}}.5$, $\delta = -59^{\circ} 14' 50''$ has been degraded by radial residual sidelobes from the $S \approx 1.3 \text{ Jy}$ background source PKS 0443–59 at J2000 $\alpha = 04^{\text{h}} 44^{\text{m}} 14.^{\text{s}}.4$, $\delta = -59^{\circ} 24' 53''$. The rms image fluctuation near NGC 1672 is $\sigma_1 \approx 40 \mu\text{Jy beam}^{-1}$. The intensity scale bar goes from -0.1 to $+10 \text{ mJy beam}^{-1}$. Right panel: The probability distribution $P(\sigma_1)$ of Stokes I image fluctuations σ_1 among the 122 snapshot observations starts near the rms thermal noise $\sigma_1 \approx \sigma_V = 14 \mu\text{Jy beam}^{-1}$ and has a long positive tail caused by residual sidelobes of strong sources in the primary beam.

We define dynamic range (DR) as the ratio of the image peak flux density to the rms image fluctuation in a source-free region near the target. Two of our 122 fields are centered on target sources with peak flux densities $S \sim 3 \text{ Jy beam}^{-1}$. NGC 1068 is near the celestial equator so its aperture-synthesis image suffers from “equator disease” and its image has a low $\text{DR} \sim 20,000:1$. The other strong target is not near the equator and its image dynamic range is $\text{DR} \sim 30,000:1$. Strong background sources anywhere in

the primary beam can also increase image fluctuations near weak targets. For example, the unusually high $\sigma_1 \approx 40 \mu\text{Jy beam}^{-1}$ near the target galaxy NGC 1672 is dominated by residual sidelobes from the $S \approx 1.3\text{Jy}$ background source PKS 0443–59 15 arcmin to the southwest (Figure 3, left panel) even though the dynamic range of this image is $\text{DR} \gtrsim 30,000 : 1$. The right panel of Figure 3 shows that $\sim 10\%$ of the 122 images have $\sigma_1 > 25 \mu\text{Jy beam}^{-1}$; of these about half (5%) are limited by background sources. Thus the fluctuations in $\sim 5\%$ of MeerKAT snapshot observations covering faint targets or no targets at all (e.g., “blind” survey fields) are likely to be significantly degraded by residual sidelobes of strong background sources.

3 MeerKAT’s Snapshot Survey Speed

The rate $\dot{\Omega}$ at which a telescope can make a “blind” survey covering a large solid angle $\Omega \gg \Omega_{\text{pb}}$ with nearly uniform sensitivity is called the instrumental survey speed. Partially overlapping snapshot images are combined with weights proportional to the local square of their primary attenuations to make the final survey image, so the effective field-of-view (Condon et al. 1998) of a nearly Gaussian primary beam whose beam solid angle is Ω_{pb} is only

$$\Omega_{\text{FoV}} = \Omega_{\text{pb}}/2 = \frac{\pi\Theta_{1/2}^2}{8\ln 2} . \quad (4)$$

At 1.28 GHz, MeerKAT’s primary beamwidth is $\Theta_{1/2} = 67'$ (Mauch et al. 2020) and $\Omega_{\text{FoV}} = 0.71 \text{deg}^2$. If an integration time τ is needed to reach the desired rms noise σ_1 at the pointing centers, then the survey rate for uniform sensitivity is

$$\dot{\Omega} = \frac{\Omega_{\text{FoV}}}{\tau} = \frac{\Omega_{\text{pb}}}{2\tau} . \quad (5)$$

Calibration and slewing overheads for surveys of contiguous areas are usually lower than the overheads for observing widely separated target sources, so a reasonable estimate based on our snapshot observations of 122 sources is that $\tau \approx 1/3 \text{ hr}$ (including overheads) for a 1.28 GHz MeerKAT survey to reach $\sigma_1 \approx 14 \mu\text{Jy beam}$. Then

$$\dot{\Omega} \approx \frac{0.71 \text{deg}^2}{1/3 \text{hr}} \left(\frac{\sigma_1}{14 \mu\text{Jy beam}^{-1}} \right)^2 \approx \left(\frac{\sigma_i}{10 \mu\text{Jy beam}^{-1}} \right)^2 \text{deg}^2 \text{hr}^{-1} . \quad (6)$$

For example, Equation 6 indicates that MeerKAT could survey $\Omega = 30 \text{deg}^2$ of sky with uniform sensitivity $\sigma_1 = 20 \mu\text{Jy beam}^{-1}$ at 1.28 GHz in a single 8 hr observing session.

References:

- Condon, J. J.; Cotton, W. D.; Greisen, E. W. et al. 1998, AJ, 115:1693
 Mauch, T.; Cotton, W. D., Condon, J. J. et al. 2020, ApJ, 888:61
 Sanders, D. B.; Soifer, B. T.; Elias, J. H. et al. 1988, ApJ, 325:74